Effect of the Substitution Ba ↔ Sr on the Ga-1222 Superstructure: An Electron Diffraction Study

O. Milat

Institute of Physics of the University, Bijenicka 46, HR-41001 Zagreb, Croatia

G. Van Tendeloo and S. Amelinckx

EMAT, University of Antwerp (RUCA), Groeneborgerlaan 171, B-2020 Antwerpen, Belgium

A. J. Wright and C. Greaves*

School of Chemistry, University of Birmingham, Birmingham B15 2TT, England

Received April 25, 1995. Revised Manuscript Received July 5, 1995[⊗]

The superstructure of the $RE_2(Sr_{0.85-x}Ba_xNd_{0.15})_2GaCu_2O_9$ compound is found to change significantly with increasing substitution of Ba for Sr. Most of the changes take place in the $(Sr_{0.85-x}Ba_xNd_{0.15})O-GaO-(Sr_{0.85-x}Ba_xNd_{0.15})O$ lamella, the rest of the basic structure being hardly affected. The structural changes for $0 \leq x \leq 0.65$ are studied by electron diffraction. The arrangement of the chains of GaO_4 tetrahedra in the Ba-free compound becomes disordered at $x > 0.25$. At $x \sim 0.65$ a rearrangement of the chains in the GaO layers takes place; they form a meandering arrangement, which can be described on a $4a_p \times 2a_p \times c_p$ superlattice. This rearrangement is accompanied by ordering of Ba and Sr atoms in the adjacent $(Sr_{0.85-x}Ba_xNd_{0.15})O$ layers. A simple scheme is proposed to explain the influence of the substitution of Ba for Sr on the linking of the GaO_4 tetrahedra and on the geometry of the "chains" in the GaO layer.

Introduction

Superconducting cuprate compounds are known to be tolerant in accepting various substitutions of aliovalent ions without profound changes to their basic structural properties; changes in the oxygen order as well as the superconducting properties can be strongly affected, however. The Cu atoms in the CuO chain layers of the $YBa_2Cu_3O_{7-x}$ compound can be completely replaced by Ga, Co, or Al atoms[1-4] and even partially by the oxyanions CO_3^{2-}, SO_4^{2-}, PO_4^{3-}, and NO_3^-,[5-8] provided that the replacement is accompanied by the simultaneous substitution of Sr for Ba ions in the adjacent rocksalt (RS) type layers. Owing to the strong tendency of M atoms (M = Ga, Co, Al) to be tetrahedrally coordinated by oxygen atoms, various MO_4 tetrahedra arrangements were found to induce different superstructures[9-12] in these compounds.

We have previously reported the structure of the phase $(Nd_{0.75}Ce_{0.25})_2(Sr_{0.85}Nd_{0.15})_2GaCu_2O_{9+\delta}$ and demonstrated the presence of GaO layers containing chains of GaO_4 tetrahedral units.[13] This general formula is abbreviated to Ga-1222, where the numbers correspond to the cation ratios in the formula. In the present paper we present the results of an electron diffraction study of the structural changes which are caused by the partial replacement of Sr by Ba to form $(Nd_{0.75}Ce_{0.25})_2(Sr_{0.85-x}Ba_xNd_{0.15})_2GaCu_2O_{9+\delta}$ with $0 \leq x \leq 0.65$.

Experimental Section

Materials with composition $RE_2(Sr_{0.85-x}Ba_xNd_{0.15})_2GaCu_2O_{9+\delta}$ were prepared by repeated heat treatments (1100 °C for 24 h in oxygen) of intimate mixtures of high-purity oxides or carbonates of the constituent metals. Samples covering the full composition range $0 \leq x \leq 0.85$ were obtained with high levels of purity. There is therefore a marked difference between the substitution properties of these Ga-1222 materials with double RE layer in the fluorite-like lamella, compared with the single RE layer Ga-1212 compounds $RESr_2GaCu_2O_7$, for which very little substitution of Ba for Sr is possible. The structures of all compounds were examined by X-ray diffraction (Siemens D5000), some by powder neutron diffraction (Polaris diffractometer, Rutherford Appleton Laboratory), and three were selected for a detailed electron diffraction study using JEOL 4000EX and Philips CM20 microscopes: $x = 0$ ("pure

[⊗] Abstract published in *Advance ACS Abstracts,* August 15, 1995.

(1) Roth, G.; Adelmann, P.; Heger, G.; Knitter, R.; Wolf, Th. *J. Phys. I* **1991**, *1*, 721.
(2) Vaughey, J. T.; Thiel, J. P.; Hasty, E. F.; Groenke, D. A.; Stern, C. L.; Poeppelmeier, K. R.; Dabrowski, B.; Radaelli, P.; Mitchell, W. A.; Hinks, D. G. *Chem. Mater.* **1991**, *3*, 935.
(3) Huang, Q.; Cava, R. J.; Santoro, A.; Krajewski, J. J.; Peck, W. F., Jr., *Physica C* **1992**, *193*, 196.
(4) Cava, R. J.; Zandbergen, H. W.; Krajewski, J. J.; Peck, W. F., Jr.; Hessen, B.; Van Dover, R. B.; Cheong, S. W. *Physica C* **1992**, *198*, 27.
(5) Slater, P. R.; Greaves, C.; Slaski, M.; Muirhead, C. M. *Physica C* **1993**, *208*, 193.
(6) Miyazaki, Y.; Yamane, H.; Ohnishi, N.; Kajitani, T.; Hiraga, K.; Morii, Y.; Funashaki, S.; Hiroi, T. *Physica C* **1992**, *198*, 7.
(7) Krekels, T.; Milat, O.; Van Tendeloo, G.; Van Landuyt, J.; Amelinckx, S.; Slater, P. R.; Greaves, C. *Physica C* **1993**, *210*, 439.
(8) Maignan, A.; Hervieu, M.; Michel, C.; Raveau, B. *Physica C* **1993**, *208*, 116.
(9) Krekels, T.; Milat, O.; Van Tendeloo, G.; Amelinckx, S.; Babu, T. G. N.; Wright, A. J.; Greaves, C. *J. Solid State Chem.* **1993**, *105*, 313.
(10) Milat, O.; Krekels, T.; Van Tendeloo, G.; Amelinckx, S. *J. Phys. I* **1993**, *3*, 1219.
(11) Zang, J. P.; Zang, H.; Dravid, V. P.; Marks, L. D.; Groenke, D. A.; Vaughey, J. T. Poeppelmeier, K. R.; Dabrowski, B.; Hinks, D. G.; Mitchell, W. A. In *Electron Microscopy I*; Kuo, K. H., Zhai, Z. H., Eds.; World Scientific: Singapore, 1992; p 252.
(12) Milat, O.; Krekels, T.; Amelinckx, S.; Greaves, C.; Wright, A. J. *Physica C* **1993**, *217*, 444.
(13) Wright, A. J.; Jennings, R. A.; Greaves, C. *Superconduct. Sci. Technol.* **1993**, *6*, 514.

0897-4756/95/2807-1709$09.00/0

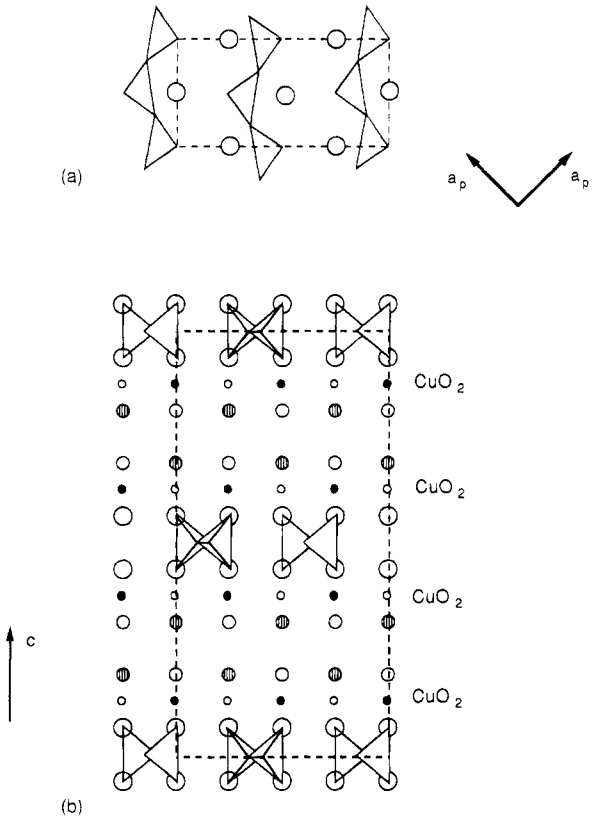

Figure 1. Schematic representation of the structure of $RE_2(Sr_{0.85-x}Ba_xNd_{0.15})_2GaCu_2O_9$. (a) View of the GaO layer along the $[001]_p$ axis. (b) View along the $[110]_p = [010]_0$ direction, revealing the stacking of the layers. Copper positions are indicated by the smallest symbols, medium circles indicate the RE ions, while the Ga and Sr ions are represented by larger circles.

Sr" compound), $x = 0.25$ ("low Ba" compound) and $x = 0.65$ ("high Ba" compound).

Structural Considerations

The basic structure of the Ga-1222 compounds can be represented by the layer stacking sequence

$$...-GaO-(Sr_{0.85-x}Ba_xNd_{0.15})O-CuO_2-RE-O_2-RE-CuO_2-(Sr_{0.85-x}Ba_xNd_{0.15})O-...$$

The thickness of this slab is 1.41 nm, while the repeat distances within a slab are determined by the basic perovskite square mesh with parameters $a_p \times a_p$ (a_p = 0.39 nm). The presence of the RE–O_2–RE fluorite-like lamella causes a lateral shift over $1/2[110]_p$ of the two parts on either side of the lamella (Figure 1). The repeat distance along the normal to the layers thus contains two such slabs and the resulting basic lattice has a body centered tetragonal cell $a_p \times a_p \times c_p$ ($c_p = 2 \times 1.41$ nm).

In the GaO layers of pure-Sr Ga-1222, the GaO_4 tetrahedra form chains of corner sharing tetrahedra along one of the two equivalent $[110]_p$ directions (Figure 1a).[1–3,9] This is in contrast with the "chains" of the square-planar CuO units running along the perovskite $[010]_p$ direction in the related Cu-1212 (or 1–2–3) structure. Due to the formation of these tetrahedral chains, an orthorhombic B-centered lattice $a_0 \times b_0 \times c_0$ was found in the Ga-1212 compounds of the type $RESr_2GaCu_2O_7$ (a_0 = 0.553 nm, b_0 = 0.545 nm, c_0 = 2.28 nm).[1,2] More complicated superstructures were recently found in the series of Ga-12n2 phases for n = 2, 3, ... (n equals the number of RE layers).[9,10] These superstructures are induced by a regular alternation of left (L) and right (R) chains along the a_0 axis (chains run parallel to b_0); the superstructure cell $a_s \times b_s \times c_s$ is 2 times larger ($a_s = 2a_0$, $b_s = b_0$, $c_s = c_0$). Twin variants were frequently found[9] since the GaO chains run along the b_0 axis which may be parallel either to the $[110]_p$ direction or to the perpendicular $[1\bar{1}0]_p$ direction in successive GaO layers.[9,10] No compositional ordering is reported so far in the adjacent layers.

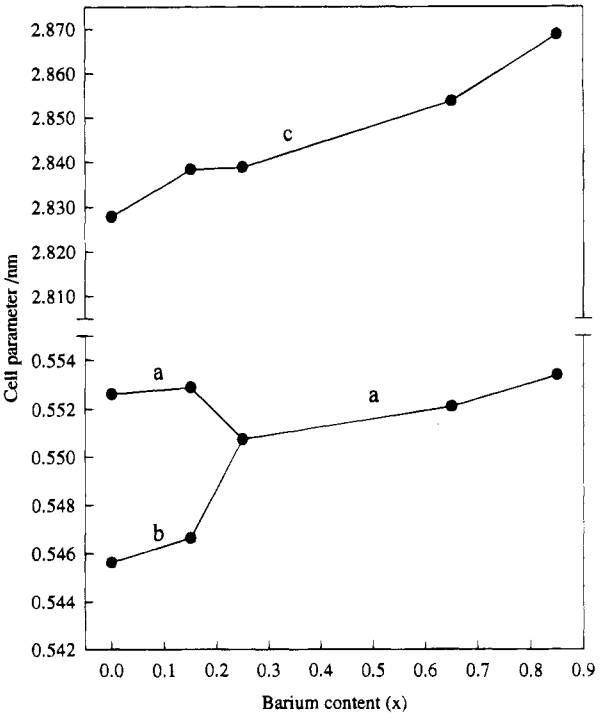

Figure 2. Change in unit-cell dimensions with Ba content x. For the tetragonal samples the a/b dimension has been multiplied by $\sqrt{2}$ to allow comparison with the orthorhombic a and b values.

The $x = 0$ sample, $(Nd_{0.75}Ce_{0.25})_2(Sr_{0.85}Nd_{0.15})_2Ga-Cu_2O_{9+\delta}$, was previously shown to be orthorhombic with a = 0.5526 nm, b = 0.5456 nm, c = 2.8279 nm.[13] The gradual replacement of Sr by Ba was found to cause a decrease in the orthorhombic distortion, and for $x \geq 0.25$ a tetragonal structure was obtained as shown in Figure 2. Although neutron diffraction data confirmed this transition, structure refinement was unable to establish the nature of the changes occurring. Given that neutron diffraction provides information only about the average unit cell within the bulk structure, a detailed examination using electron diffraction was performed on three samples with $x = 0$, $x = 0.25$, and $x = 0.65$.

Electron Diffraction Results

The [001] diffraction patterns of three Ga-1222 compounds with different levels of (Ba ↔ Sr) substitution are shown in Figure 3; a series of $[hk0]$ zone patterns for "pure-Sr", "low-Ba", and "high-Ba" Ga-1222 crystals are shown in Figures 4–6, respectively. These patterns allow reconstruction of the complete reciprocal lattices.

The most intense spots in all patterns are those generated by the basic perovskite structure. Due to the extinction condition $h_p + k_p + l_p$ = odd, the basic spots

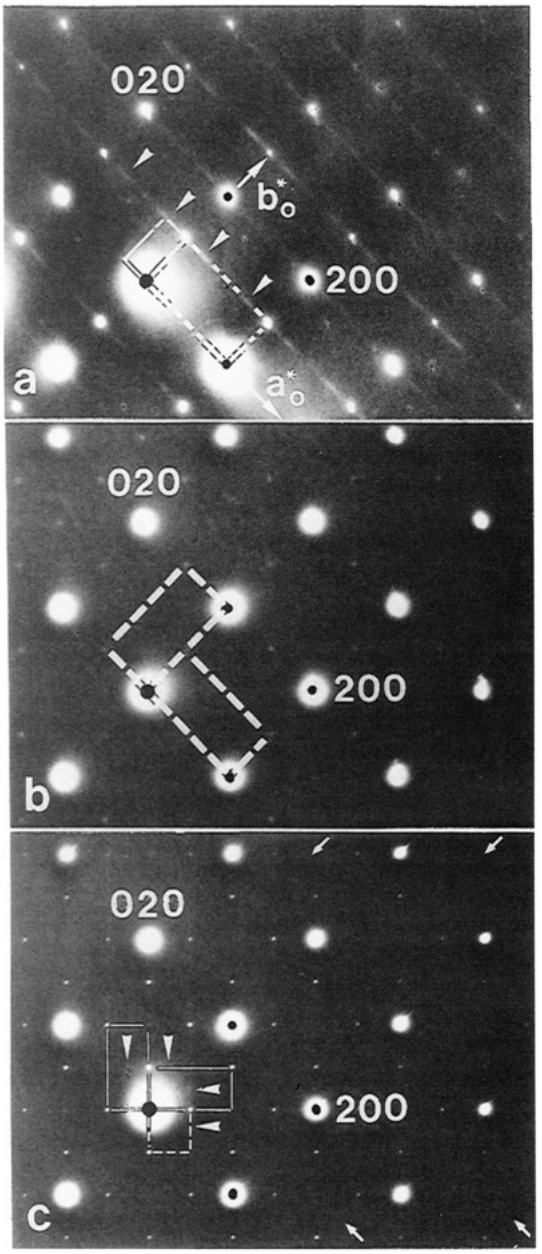

Figure 3. Diffraction patterns of $RE_2(Sr_{0.85-x}Ba_xNd_{0.15})_2GaCu_2O_9$ along the [001] zone. (a) $x = 0$; (b) $x = 0.25$; (c) $x = 0.65$. The outlined cells in (a) and (b) correspond to the orthorhombic lattice $a_0 \times b_0$; the broken square in (c) marks the unit cell the $2a_p \times 2a_p$ lattice. The full line rectangle in (a) indicates the reciprocal mesh of the $2a_0 \times b_0$ superlattice, while the full lines in (c) mark the C-centered meshes of two variants of the $4a_p \times 2a_p$ superlattice. Arrowheads in (a) and (c) mark the spots which represent the intersections of diffuse streaks visible in Figures 3 and 5, respectively.

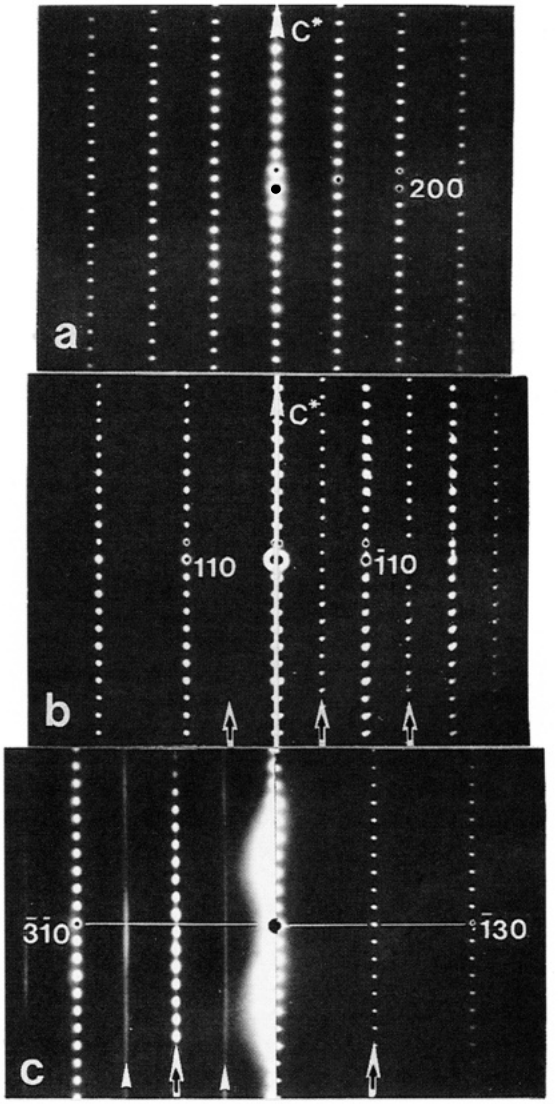

Figure 4. Series of diffraction patterns of the "pure Sr" compound; the basic reflections are marked by black dots and labeled in the perovskite notation: (a) the $[010]_p$ zone; (b) the $[110]_p$ zones; the left and the right part represent the $(0kl)_0^*$ and the $(h0l)_0^*$ sections; (c) the $[310]_p$ zone where the left and right part represent the $(h\ 2h\ l)_0^*$ and the $(2k\ k\ l)_0^*$ sections, respectively.

can be indexed on a face-centered reciprocal cell which is approximately tetragonal, regardless of the Ba/Sr composition. This is in agreement with the body centered cell of the basic Ga-1222 structure (Figure 1).

Besides the basic spots (marked by black dots in Figure 3), different weak superstructure reflections are observed, depending on the level of the Ba/Sr substitution (Figure 3). The relatively intense superstructure reflections at $^1/_2\ ^1/_2\ 0$ positions (Figure 3a) are consistent with the B-face centered orthorhombic cell: $a_0 \times b_0 \times c_0$.[1] The mesh of basic spots in Figure 3a is not prefectly square, as it is in Figure 3b,c; this relates to the fact that $a_0 > b_0$ which makes the angle between $[100]_p^*$ and $[010]_p^*$ different from 90°. The very weak and diffuse spots, marked by arrowheads in Figure 3a and situated at $\pm^1/_2 a_0^*$ determine a smaller reciprocal unit mesh of $^1/_4 d^*_{1\bar{1}0} \times {}^1/_2 d^*_{110p}$ (marked by a full line rectangle), which in real space corresponds to a superstructure with lattice parameters $a_s = 2a_0$, $b_s = b_0$, $c_s = c_0$.[9,10] Note that no traces of these reflections are present in Figure 3b.

The pattern of sharp but weak superlattice spots in Figure 3b consists of two overlapping rectangular meshes, each of them being analogous to the sharp spot mesh in Figure 3a but rotated through 90° with respect to each other. The slight difference in superstructure intensity of both sublattices proves the presence of twin related variants. In Figure 3b there is no longer a measurable difference between the basic spot spacing, indicating that the basic sublattice is undistorted; the orthorhombic lattice parameters a_0 and b_0 become equal.

The superlattice configuration in Figure 3c is quite different from that in Figure 3a,b. The square mesh $^1/_2 d^*_{100p} \times {}^1/_2 d^*_{010p}$, indicated by dotted lines, reveals a

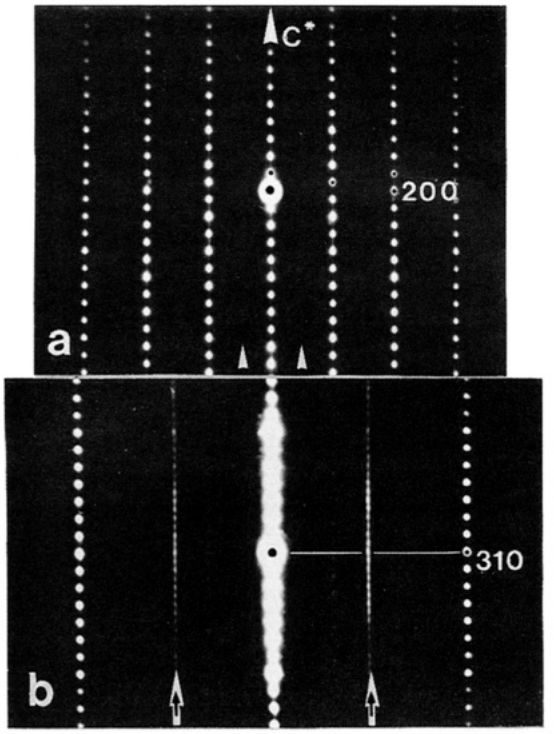

Figure 5. Diffraction patterns of the "low-Ba" compound: (a) the $[100]_p$ zone; (b) the $[130]_p$ zone.

$2a_p \times 2a_p$ superlattice with the axes along the principal perovskite directions. Additional, extremely weak and diffuse scattering, marked by arrowheads at positions $\pm^1/_4 d^*_{010p}$ around the superlattice spots along the $[100]_p^*$ axis, can be interpreted as belonging to two weakly centered rectangular meshes, indicated by full lines in Figure 3c. This interpretation is confirmed by careful tilting experiments (Figure 6), where weak streaks were found to be associated with these positions. The superstructure reflections reveal an additional ordering in the "high-Ba" Ga-1222 structure, which can be described in a $4a_p \times 2a_p$ superlattice.[12]

The tilt series around the [001] axis for the "pure-Sr" compound (Figure 4) can be indexed on the B-face centered orthorhombic unit cell ($a_0 \times b_0 \times c_0$), as well as on the superlattice cell ($a_s \times b_s \times c_s$).[9,10] The rows of reflections which belong to the B-face centered orthorhombic lattice are marked by open arrows in the left and right parts of Figure 4b,c. The diffuse streaks, marked by the white arrowheads in Figure 4c cannot be indexed in the orthorhombic description; they belong exclusively to the superlattice cell.[9,10] These diffuse streaks intersect the $(hk0)^*$ section and are responsible for the diffuse points marked by arrowheads in Figure 3a.

The patterns of the "low-Ba" compound in Figure 5a,b represent the $(h0l)_p^*$ and $(3kkl)_p^*$ reciprocal sections; these are the ones which differ from the corresponding sections of the "pure Sr" compound. In Figure 5a, a faint trace of diffuse scattering (marked by arrowheads) can be discerned halfway between the basic spot rows. In the section of Figure 5b, diffuse streaking is present through the rows of spots corresponding to the orthorhombic structure (marked by open arrows); moreover the spot density is double compared to the basic spot rows or compared to the case of the "pure-Sr" compound (Figure 4c). The pattern is actually due to the overlapping of two perpendicular $[\bar{1}30]$ and [310] zone patterns, shown in the left and right parts of Figure 4c. This interpretation is consistent with the weak spot pattern of Figure 3b.

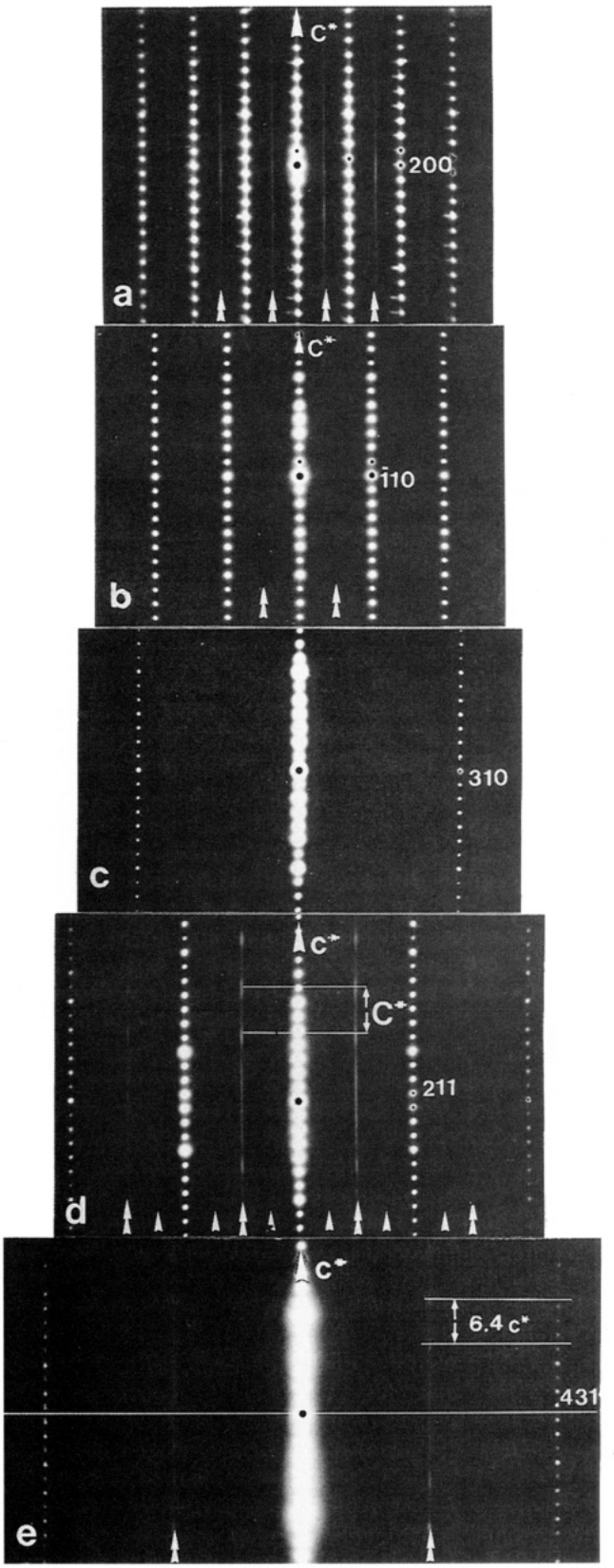

Figure 6. Diffraction patterns of the "high-Ba" compound: (a) the $[010]_p$ zone; (b) the $[110]_p$ zone; (c) the $[130]_p$ zone; (d) the $[120]_p$ zone; (e) the $[340]_p$ zone. Double arrowheads in (a), (b), (d), (e) mark the diffuse streaks which belong to the $2a_p \times 2a_p$ network; single arrowheads in (d) mark the very weak streak which belong to the centered $4a_p \times 2a_p$ network.

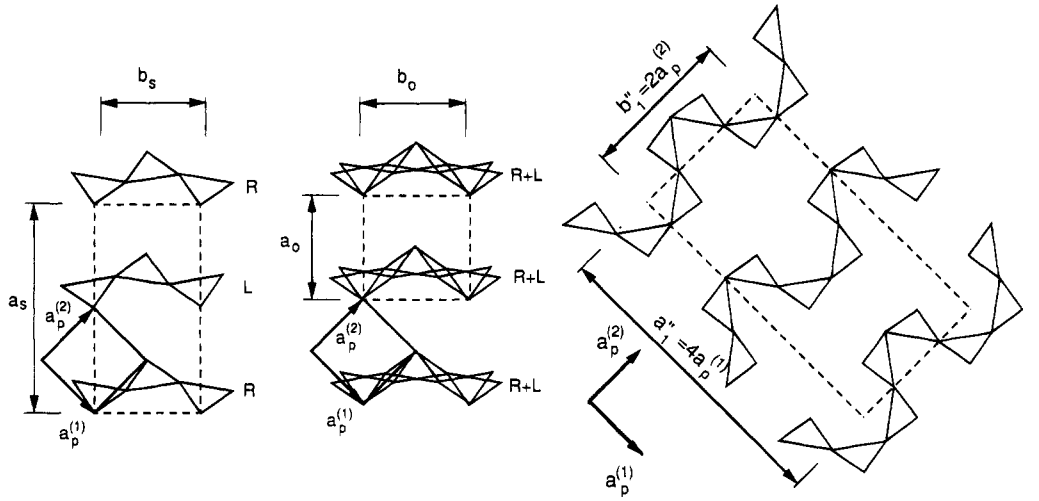

Figure 7. Tetrahedral chain configuration in the GaO layer of the $RE_2(Sr_{0.85-x}Ba_xNd_{0.15})_2GaCu_2O_9$ structure: (a) $x = 0$, with the $2a_0 \times a_0$ superstructure cell; (b) $x = 0.25$, with the $a_0 \times a_0$ cell; (c) $x = 0.65$, where the $4a_p \times 2a_p$ superstructure cell is marked.

The patterns of the "high-Ba" compound in Figure 6 represent a tilt series which besides the basic reflections reveal diffuse streaks of two different types, leading to the superstructures $2a_p \times 2b_p \times c_p$ and $4a_p \times 2b_p \times c_p$ defined before. The streaks, marked by double arrowheads in Figure 6a,b,d,e, exhibit a clear intensity modulation along c^*. The period of this sinusoidal modulation is $C^* \sim 6.4c_p^*$. This C^* period indicates a bilayer correlation within the unit slab in direct space.[14] The corresponding real-space modulation period of $1/C^* \sim 0.44$ nm suggests that the correlated bilayer in the Ga-1222 structure is the $(Sr_{0.85-x}Ba_xNd_{0.15})O$ bilayer. These related streaks in reciprocal space intersect the Ewald's sphere in the $(hk0)^*$ section at the $(1/2\ 1/2\ 0)_{4\times2}$ position in Figure 3c. The streaks of very weak intensity (marked by single arrowheads in Figure 6d) intersect the Ewald sphere at the centers of either of the two rectangular meshes in Figure 3c.

Discussion

GaO Chain Arrangement for $x \leq 0.25$. The superstructure of the "pure-Sr" Ga-1222 phase is characterized by the formation of chains of corner-sharing GaO_4 tetrahedral in the GaO layers, the other layers being hardly affected.[9,10] The superlattice cell $a_s \times b_s \times c_s$ can be attributed to an antiparallel arrangement of "left" and "right" chains (Figure 7a). If no distinction between "left" and "right" is taken into account, an apparent average chain structure, based on the smaller B-face centered orthorhombic cell $a_0 \times b_0 \times c_0$ would result (Figure 7b). More structural details on this superstructure (in a 1212 type structure) are given in ref 9. The antiparallel alignment of all GaO_4 chains in all GaO planes along the same $[110]_p$ axis seems to be responsible for the observed 2% difference between the a_0 and the b_0 orthorhombic cell parameters.[1]

The increasing level of Ba for Sr substitution at $x = 0.25$ in the "low-Ba" compound leads to the disappearance of the antiparallel GaO chain superstructure. This can be caused either by an accommodation of the Ga and/or O atoms in the special positions (which would eliminate the "left" and "right" feature of the GaO chains[9]) or by preserving this directional chain feature only locally over very small dimensions.

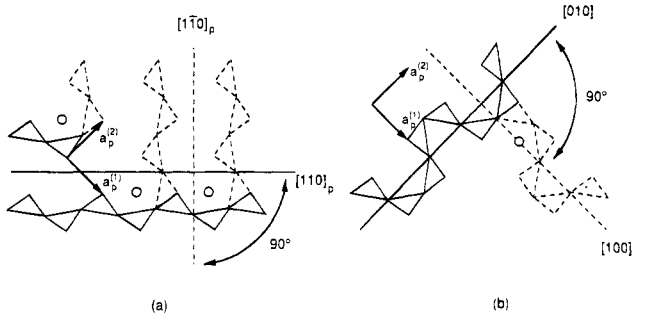

Figure 8. Schematic representation of the 90° orientation changes in the tetrahedral chains: (a) for the $x = 0$ or $x = 0.25$ compound; (b) for the $x = 0.65$ compound with meandering chains. Full and dotted tetrahedra run along two mutually perpendicular directions.

The influence of a Ba atom substitution for a Sr atom on this disordering can be understood from the following scheme:

Each Ba atom replacing a Sr atom acts as a "Ba-associated defect" in the (Sr/Ba)O layer surrounding the GaO layer, it may influence the local linking of two neighboring GaO_4 tetrahedra in a way to induce a change in the chain direction and/or to affect the chain orientation.[9]

When a "Ba-associated defect" affects the chain orientation, the chain becomes fragmented in parts along the $[110]_p$ axis and parts along the perpendicular $[1\bar{1}0]_p$ axis (Figure 8a). The higher the defect concentration, the more frequent the change in orientation. These changes in orientation only affect the GaO layers. The presence of such faulted layers induces a mixing of B-centered and A-centered structures.[9] Heavy disorder of these chain directions and changes of orientation for higher levels of Sr/Ba substitution will introduce an average tetragonal symmetry and destroy the orthorhombic symmetry present in the "pure Sr" compound. This is indeed observed in the diffraction patterns of Figures 3b and 5b.

Meandering GaO Chains. The idea of a "Ba-associated defect" can be further used to explain the formation of a meandering GaO chain configuration in the "high Ba" compound. For a high defect configura-

(14) Verwerft, M.; Van Tendeloo, G.; Van Landuyt, J.; Amelinckx, S. *Appl. Phys.* **1990**, *A51*, 332.

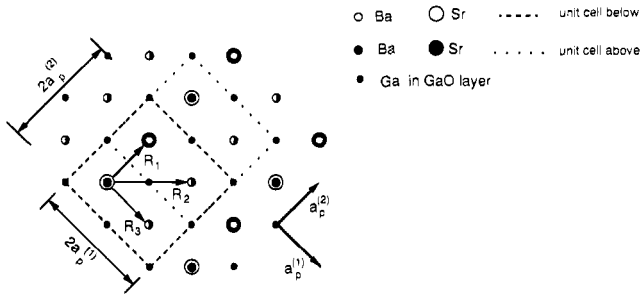

Figure 9. Compositional ordering in the (Sr/Ba)O planes of the (Sr/Ba)O–GaO–(Sr/Ba)O lamella for the $x = 0.65$ compound. Open and closed symbols are in the upper and lower (Sr/Ba)O plane, respectively. R_i mark the planar components of the displacement between top and bottom layer.

tion, i.e., for a Ba/Sr ratio roughly equal to 3/1, the induced changes in chain orientation take place practically at each and every neighboring site. Consequently, segments of two GaO_4 tetrahedra along the $[110]_p$ axis regularly alternate with segments of two tetrahedra oriented along the perpendicular $[1\bar{1}0]_p$ axis. The corresponding superstructure can be described on a $4a_p \times 2a_p \times c_p$ lattice (Figure 7c). Such a meandering chain arrangement was also found in the AlO chain layer of the "pure Sr" Al-1222 structure.[12] The meandering chains run along either of the two principal perovskite directions $[100]_p$ or $[010]_p$. When point defects are introduced—either in the GaO plance or in the adjacent (Ba/Sr)O planes—the meandering chain may change orientation by 90°. Two perpendicular meandering chain directions (90° twins) may coexist, even within a single (Ba/Sr)O–GaO–(Ba/Sr)O lamella. This was observed in the Al-1222 structure.[12]

Compositional Ordering within the (Sr/Ba)O Bilayers. For high Ba-containing compounds ($x = 0.65$), the idea of a "Ba-associated defect" has to be slightly adapted in order to explain the modulation period of 0.44 nm along c^* (Figure 6). In the basic Ga-1222 structure only the (Sr/Ba/Nd)O bilayer has an interlayer spacing of 0.44 nm and is therefore to be associated with the modulation. A simple scheme of composition ordering of 3 Ba and 1 Sr atoms on a $2a_p \times 2a_p$ lattice is shown in Figure 9; the stacking of both $(Sr_{0.25}Ba_{0.75})O$ layers is hereby also schematized. Since the intensity of the streaks in Figure 6e have a minimum at $l = 0$, the occurrence of a vertical stacking of the meshes in the consecutive $(Sr_{0.25}Ba_{0.75})O$ layers is unlikely. The relative displacement vector R_1 in Figure 9 represents one possible configuration of Ba and Sr atoms on the $2a_p \times 2a_p$ lattice in the $(Sr_{0.25}Ba_{0.75})O$ layer below and above the GaO chain plane. Other configurations with displacement vectors R_2 or R_3 are equally consistent with the intensity minimum at $l = 0$. The stacking of this bilayer in successive slabs is correlated by one of the vectors $R = \pm{}^1/_2a_p \pm {}^1/_2a_p + {}^1/_2c_p$, generating the observed extinction conditions for the superlattice spots in the $(hk0)^*$ section of Figure 3c.

Meandering Chain Configurations in the (Ba/Sr)O–GaO–(Ba/Sr)O Lamella. In contrast to the strictly C-centered cell of the meandering chain structure in the Al-1222 phase,[12] the reciprocal cell of the "high-Ba" Ga-1222 phase is only weakly C-centered (Figure 3c). The model of the meandering chain structure in the AlO layer[12] has to be modified here to take into account the larger size of the Ga versus the Al ion.

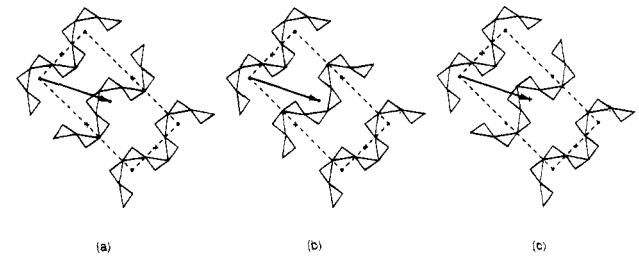

Figure 10. Three configurations of meandering GaO_4 chains on the two dimensional $4a_p \times 2a_p$ supercell. In (a) a C-centered arrangement results, while in (b) and (c) a primitive cell is formed. In (a) all chains are identical but successive chains are shifted in phase. In (b) successive chains are related by a glide mirror operation. In (c) chains are related by a mirror operation.

The corner-sharing GaO_4 tetrahedra do not fit the perovskite mesh without an accommodating displacement of the Ga and O atoms out of their special positions.[9] As a consequence several meandering chain configurations may be considered (Figure 10). We can only speculate about the mutual interaction between the configuration in the (Sr/Ba)O bilayer and the meandering chain arrangement in the sandwiched GaO layer. However, pursuing the simple model of the Ba/Sr ordering on a $2a_p \times 2a_p$ mesh in the (Sr/Ba)O layers, the geometry of the strictly C-centered $4a_p \times 2a_p$ mesh of Figure 10a can be regarded as less favourable than the geometry of primitive meshes, shown in Figure 10b,c. The configurations based on the primitive $4a_p \times 2a_p$ mesh in Figure 10b or on the $4a_p \times 2a_p$ mesh in Figure 10c are more likely to fit the $2a_p \times 2a_p$ meshes in the surrounding layers. Actually, these different arrangements could locally coexist in the GaO layers, causing a weak C-centering and a lack of order along the $a_s = 4a_p$ superlattice axis.

Conclusions

Depending on the level of Ba for Sr substitution, the structure of the $RE_2(Sr_{0.85-x}Ba_xNd_{0.15})_2GaCu_2O_{9+\delta}$ phases can adopt various superstructures. In the "pure-Sr" compound the corner-sharing GaO_4 tetrahedra arrange themselves in antiparallel chains within the (Sr/Nd)O–GaO–(Sr/Nd)O lamella. A slight deformation of the square perovskite mesh (decrease in the angle between $[100]_p$ and $[010]_p$) causes the spacing along the chains to be shorter then the spacing perpendicular to the chains.

The increasing level of Ba for Sr substitution in the $(Sr_{0.85-x}Ba_xNd_{0.15})O$ layers ($x \leq 0.25$) induces a fragmentation of the GaO chains and disordering of the chain directions. The orthorhombic structure is locally preserved due to a predominant alignment of neighboring chains containing both "left" and "right" fragments, but the size of the domains decreases. The chains frequently change their orientation by 90°, which results in a mixing of domains and structural disorder. The individual layers behave in a way that is not correlated with the neighboring layers. The parameters a_0 and b_0 of such "average" cell become equal in length and the apparent symmetry is enhanced to the tetragonal one of the perovskite structure.

At a high level of Ba for Sr substitution ($x = 0.65$) an arrangement of "meandering" GaO_4 chains is formed, which can be described on a $4a_p \times 2a_p \times c_p$ lattice. The

meandering chain arrangement can be regarded as an ordered configuration of segments of two corner-sharing GaO_4 tetrahedra, whose directions and orientations alternate regularly at each neighboring site in the GaO layer. Such arrangements appear in two orientation variants, without deformation of the basic perovskite lattice. The disordering of such arrangements results in an "average" structure with apparent tetragonal symmetry.

At particular levels of Ba for Sr substitution ($x = 0.25$ and $x = 0.75$) a compositional ordering of Ba and Sr atoms in the $(Sr_{0.85-x}Ba_xNd_{0.15})O...(Sr_{0.85-x}Ba_xNd_{0.15})O$ bilayers can take place on a two-dimensional lattice described on a $2a_p \times 2a_p$ unit cell. Such ordering was found to accompany the "meandering" GaO chain arrangement.

Acknowledgment. O. Milat is grateful to DG XII of the EC Commission for financial support during his research stay at EMAT-RUCA. This work has been performed within the framework of the Belgian Impulse Program SU/03/17 and with financial support of the Ministery of Science, Republic of Croatia. A.J.W. and C.G. are grateful for financial support from EPSRC.

CM950186E